ResearchGate

See discussions, stats, and author profiles for this publication at: https://www.researchgate.net/publication/239937758

# A record of post-glacial moraine deposition and tephra stratigraphy from Otokomi Lake, Rose Basin, Glacier National Park, Montana

**Article** *in* Canadian Journal of Earth Sciences · April 2006

Impact Factor: 1.58 · DOI: 10.1139/E06-001

CITATIONS
3

READS
38

**3 authors**, including:

Ian S Spooner
Acadia University

**50** PUBLICATIONS **295** CITATIONS

SEE PROFILE

All in-text references underlined in blue are linked to publications on ResearchGate, letting you access and read them immediately.

Available from: Ian S Spooner
Retrieved on: 13 May 2016

# A record of post-glacial moraine deposition and tephra stratigraphy from Otokomi Lake, Rose Basin, Glacier National Park, Montana

**David Matthew MacLeod, Gerald Osborn, and Ian Spooner**

**Abstract:** The sedimentary record of Otokomi Lake, Glacier National Park, Montana, was studied to determine the age of an adjacent Crowfoot moraine. The presence of Mt. St. Helens Jy ash near the bottom of the longest percussion core limits drainage basin deglaciation to before 11 400 $^{14}$C years before present (BP), although 14 100 BP is the estimated basal age of the core. Correlative shifts in loss on ignition, coarse (>1 mm) grain size, magnetic susceptibility, and X-ray gray-scale data at a depth of 185 cm are interpreted to be related to a sedimentary change in Otokomi Lake brought about by the deposition of the adjacent Crowfoot moraine. The estimated age of the moraine is 10 590 BP, which is within the Younger Dryas interval. This information supports the hypothesis that Crowfoot moraines represent a regional western North American response to Younger Dryas cooling.

**Résumé :** Les strates sédimentaires du lac Otokomi, dans le Glacier National Park, au Montana, ont été étudiées afin de déterminer l'âge d'une moraine Crowfoot adjacente. La présence de cendre volcanique Jy du mont Saint Helens presque au fond de la plus longue carotte obtenue par un forage à percussion signale que la déglaciation du bassin de drainage est survenue antérieurement à 11 400 années $^{14}$C avant le présent, alors que la base de la carotte a été estimée à 14 100 années $^{14}$C avant le présent. Les décalages dans les données des corrélations concernant les pertes au feu, les particules grossières (> 1mm), la susceptibilité magnétique et les niveaux de gris aux rayons X à une profondeur de 185 cm sont interprétés comme étant reliés à un changement sédimentaire dans le lac Otokomi; ce changement résulterait de la déposition de la moraine Crowfoot adjacente. L'âge estimé de la moraine est de 10 590 années $^{14}$C avant le présent, ce qui est dans l'intervalle du Dryas Récent. Cette information soutient l'hypothèse que les moraines Crowfoot représentent une réponse de l'Amérique du Nord occidental au refroidissement durant le Dryas Récent.

[Traduit par la Rédaction]

## Introduction

The Younger Dryas has been widely recognized as a cool interval, dated between 11 000 and 10 000 $^{14}$C years before present (BP), which interrupted the warm Bølling–Alleröd interval that followed the Wisconsinan Glaciation. A disruption of North Atlantic Ocean water circulation, caused by the catastrophic drainage of subglacial Lake Agassiz, is the current paradigm used to describe the cause of Younger Dryas cooling (Rind et al. 1986; Broecker et al. 1989).

The Younger Dryas cooling event persisted for ~1300 calendar years (Alley et al. 1993). Its abrupt termination was marked by a mean annual temperature increase of up to 7 °C over a period of 20–50 years (Dansgaard et al. 1989; Taylor et al. 1993; Alley et al. 1993). The geographic extent of the Younger Dryas remains a subject of debate. A mounting body of evidence supports global cooling during the Younger Dryas (Kudras et al. 1991; Scott et al. 1995; Osborn et al. 1996; Mikolajewicz et al. 1997; Rutter et al. 2000; Zhou et al. 2001; Kovanen 2002); however, some researchers have disputed this claim, offering evidence to support climate stability or even climate warming during this interval (Heine 1994; Heine and Heine 1996; Singer et al. 1998; Bennett et al. 2000).

The present study was conducted in Rose Basin, Glacier National Park, Montana (Fig. 1). A cirque at this site contains a glacial moraine that appears to be Crowfoot-equivalent in age (Osborn 1985; Carrara 1987). Crowfoot moraines were first identified by Luckman and Osborn (1979), have a geographic extent ranging from Jasper, British Columbia to Colorado (Reasoner et al. 1994; Menounos and Reasoner 1997), and may represent a period of regional glacial re-advance or a glacial still stand in response to Younger Dryas cooling. Crowfoot moraines, by definition, are overlain by Mazama ash, which constrains their deposition to pre-6730 BP (Hallett et al. 1997). Other than the type Crowfoot moraine, which has an estimated age between 11 330 and 10 100 BP (Reasoner et al. 1994), no Crowfoot moraine has been nar-

Received 23 February 2005. Accepted 10 January 2006. Published on the NRC Research Press Web site at http://cjes.nrc.ca on 4 May 2006.

Paper handled by Associate Editor R. Gilbert.

**D.M. MacLeod[1] and G. Osborn.** Department of Geology and Geophysics, University of Calgary, Calgary AB T2N 1N4, Canada.
**I. Spooner.** Department of Geology, Acadia University, Wolfville NS B0P 1XO, Canada.

[1]Corresponding author (e-mail: dmmacle2@dal.ca).

 doi:10.1139/E06-001 © 2006 NRC Canada

**Fig. 1.** Aerial photograph showing location of Rose Basin and Otokomi Lake in Glacier National Park, Montana. Photo 26A-26 courtesy of the US. Department of the Interior, taken July 27, 1968. asl, above sea level.

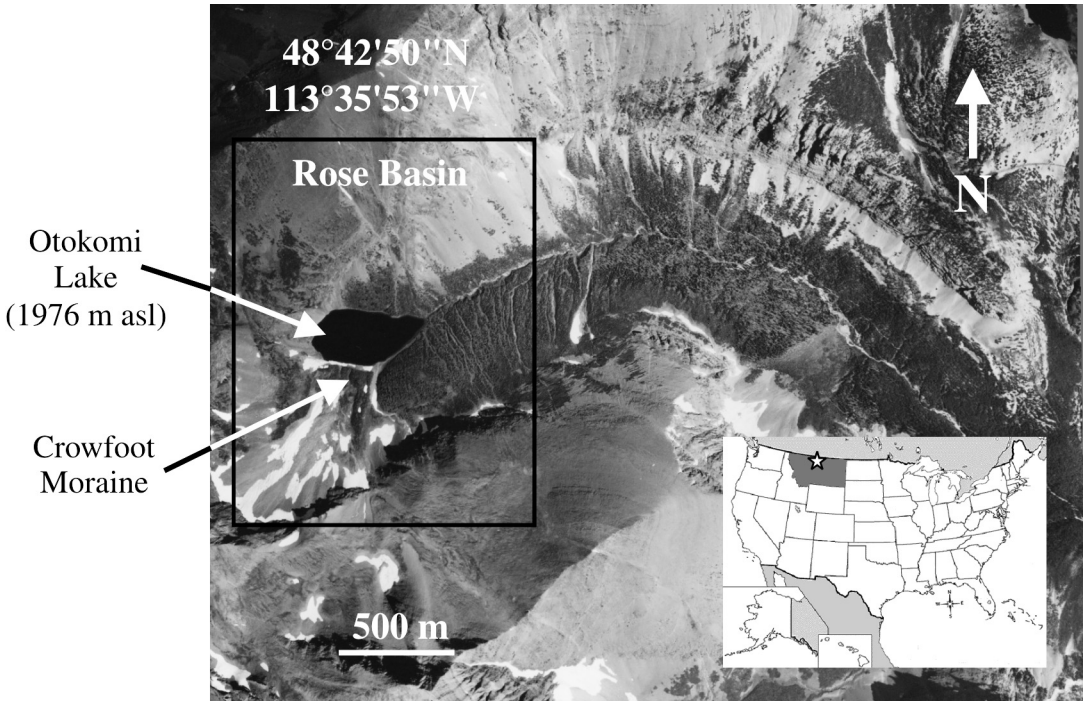


rowly bracketed in age. The purpose of the present study was to determine the age of the Crowfoot moraine in Rose Basin through lake sediment analysis.

## Previous research

### Post last-glacial-maximum glacial activity in the North American Cordillera

Several researchers have noted pre-Younger Dryas glacial activity in the post last-glacial-maximum geologic record of the North American Cordillera. This glacial activity ranges in age from 11 800 BP to11 200 BP and includes both cirque glacier activity (Davis and Osborn 1987; Zielinski and Davis 1987; Heine 1996; Clark and Gillespie 1997; Osborn and Gerloff 1997) and the advance of the Cordilleran ice sheet (Easterbrook and Kovanen 1998; Kovanen 2002). Although both the cause of these pre-Younger Dryas advances and their relation to one another are unknown, the possibility is that they represent a period of widespread glacial re-advance in the North American Cordillera.

Many paleoclimatic reconstructions in areas of the North American Cordillera that lack suspect Crowfoot moraines provide evidence for glacial activity or cool conditions during the Younger Dryas interval. Engstrom et al. (1990) demonstrated cooling in southeastern Alaska with lacustrine pollen and geochemical data. Mathewes et al. (1993) identified cool and wet conditions on the coast of British Columbia using benthic foraminifera and fossil pollen data. Gosse et al. (1995) found evidence for glacial advance in the Wind River Range of Wyoming using cosmogenic $^{10}$Be. Menounos and Reasoner (1997) provided lacustrine sedimentary evidence for glacial advance in the front range of the Colorado Rockies. Briner et al. (2002) used cosmogenic $^{10}$Be and $^{26}$Al data, in conjunction with radiocarbon dating of lacustrine sediment, to provide evidence for glacial advance in southwestern Alaska. Friele and Clague (2002) used geomorphologic evidence, in conjunction with radio carbon dating, to demonstrate the re-advance of a valley glacier in the southern Coast Mountains of British Columbia. These studies, along with that of Reasoner et al. (1994), are all part of the growing body of evidence for cool, and possibly wet, conditions during the Younger Dryas interval in western North America.

Claims of early Holocene glacial advances in the Cordillera have been debated. The Chateau Lake Louise Advance of Harris and Howell (1977) was challenged by Luckman and Osborn (1979) and is no longer believed to be early Holocene in age. Beget's (1983) "Mesoglaciation" at ca. 8000 BP, which included the then undated Crowfoot Advance, was disputed by Davis and Osborn (1987), and Osborn and Gerloff (1997). In general, most evidence related to early Holocene climate in the Canadian Rockies suggests warm conditions characterized by forest expansion and glacial retreat (e.g., Luckman and Osborn 1979; Luckman and Kearney 1986; Luckman 1988; Tomkins 2000). However, interest in a "8200-year (calendar years) cold event" recorded in Greenland ice cores (Alley et al. 1997) has lead to examination of Cordilleran records, and Menounos et al. (2004) present sedimentological evidence for a minor advance at about that time in the southern Coast Mountains of British Columbia.

The remainder of early Holocene glacial advances recognized in the North American Cordillera postdate the deposition of Mazama ash (Fulton 1971; Osborn 1986; Ryder and Thomson 1986; Osborn and Gerloff 1997), and as such, do not bear on the question of Younger Dryas cooling.

### Deglaciation of northwestern Montana and Glacier National Park

During the height of the late Wisconsinan glaciation, Glacier

© 2006 NRC Canada

**Fig. 2.** Rose Basin and Otokomi Lake. Moraine crest demarcated with dashed line and coring sites C1 and C2 indicated.

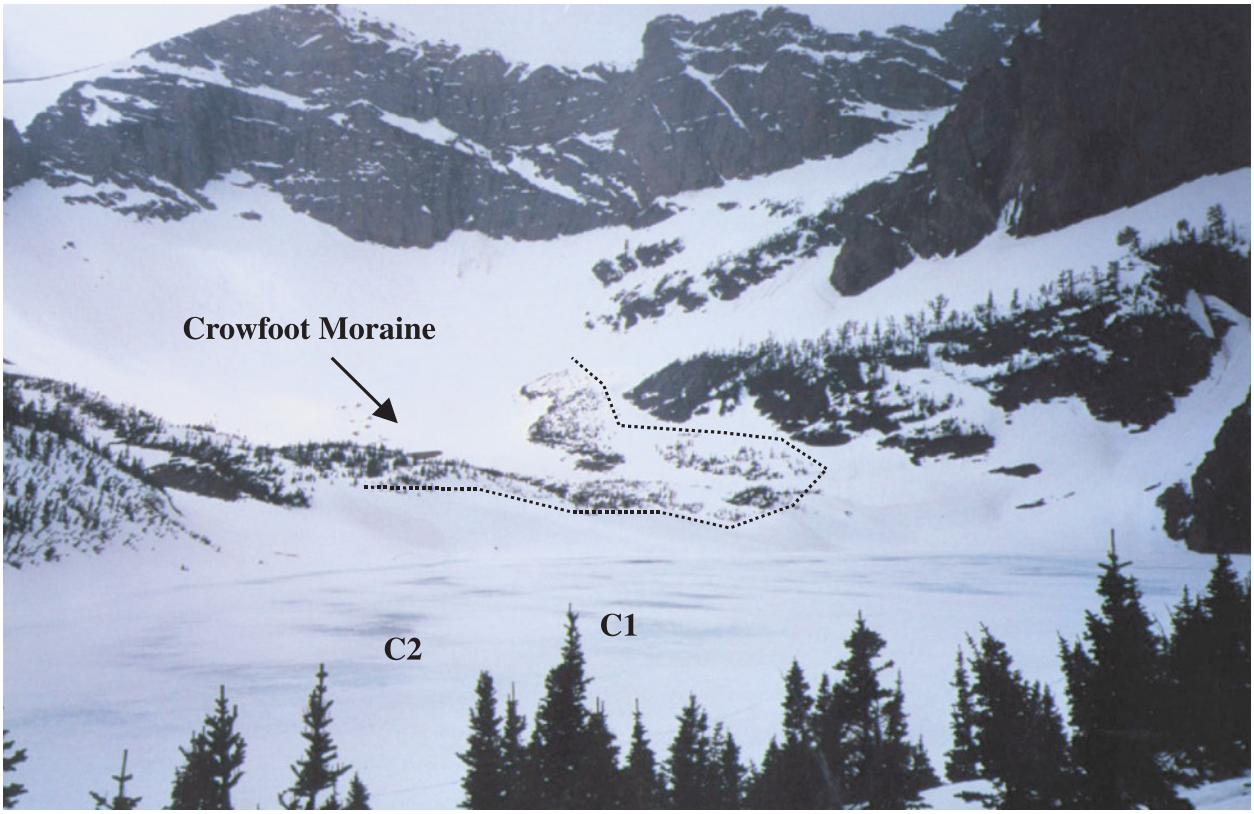


National Park was covered by ice fields and valley glaciers, bordered on the west by the Cordilleran Ice Sheet and on the east by a narrow expanse of open plains (Alden 1953; Waitt and Thorson 1983). Based on a study of late-Pleistocene sediment exposures and bog sediments, Carrara (1989) concluded that Glacier National Park was extensively deglaciated prior to 11 400 BP. This deglaciation included Marias Pass on the continental divide immediately south of the park (elevation 1595 m above sea level (asl)). In the Mission Mountains southwest of Glacier National Park, Gerloff et al. (1995) concluded that deglaciation predated 11 200 BP, based on the presence of Glacier Peak G tephra in a lacustrine sedimentary record from 1887 m asl. East of the Mission Mountains in the Sun River Canyon, Lemke et al. (1975) concluded that valley ice had retreated 11 km upvalley by 11 200 BP, based on the presence of Glacier Peak tephra in an ancient alluvial fan deposit. In the Bitterroot Mountains of west-central Montana, the sedimentary record from a bog at 2152 m asl indicates deglaciation by 12 000 BP (Mehringer et al. 1977). Based on a lake-sediment study on the Great Plains of Montana, east of Glacier National Park, it was concluded that the ice of the Two Medicine Glacier, which was fed by ice from Two Medicine Valley and Marias Pass, had retreated from the Great Plains by 12 200 BP (Barnosky 1989).

## Methods

### Site selection and coring methods

Glacier National Park Montana, was chosen as the general study area because Osborn (1985), Carrara (1987), and Carrara and McGimsey (1988) had already identified many Crowfoot moraines in its alpine environment. An air photo survey of the park revealed Rose Basin (Fig. 1) as the most appropriate site for the present study, based on the proximity of a Crowfoot moraine to a candidate lake (Otokomi Lake) and site accessibility. To characterize the sedimentation dynamics within Otokomi Lake, additional field data were gathered in the summer of 2001, which included a bathymetric sonar-survey of the lake, water temperature profiling, and a site survey to identify inlet and outlet streams within the basin.

Rose Basin (Fig. 2) is underlain by west-dipping, thrust-faulted meta-sedimentary and meta-volcanic strata of the Grinnel, Appekunny, and Empire formations. These rocks are part of the Proterozoic-aged Belt–Purcell Supergroup. Rose Creek has a late-summer discharge of ~4.52 $m^3$/min and is the only outlet from Otokomi Lake. One small inlet stream enters the lake from the southwest, from a small pond perched on bedrock cliffs. There are also several ephemeral inlet streams located around the lake's perimeter. The north shore and eastern margins of the lake are bordered by scrubby forest and herbaceous lakeshore vegetation, whereas the west end of the lake meets bedrock cliffs. A small talus slope, which originates from these cliffs, builds into the northwest end of the lake. The cirque to the south of the lake has an average headwall elevation of 2400 m and now holds only a small amount of perennial ice. The vegetated Crowfoot moraine identified by Osborn (1985) and Carrara (1987) is located at the bottom of this cirque along the lake's southern shore. The terminal portion of the moraine is ~10 m in height and 200 m long. A pit, dug into the crest of the moraine, confirmed the presence of glacial till. No obvious

© 2006 NRC Canada

**Fig. 3.** Otokomi Lake bathymetry including percussion core sites, location of the moraine, talus slope, water inflow and outflow and sample sonar echogram, A–B. Sonar reflector R1 is interpreted to be the water–sediment interface along the basin slope, R2 is interpreted to be a multiple of R1 and R3 is interpreted to be the interface between water and the profundal sediment of the basin deeps. The sonar echogram includes an overlay of the lake temperature profile, recorded August 2001.

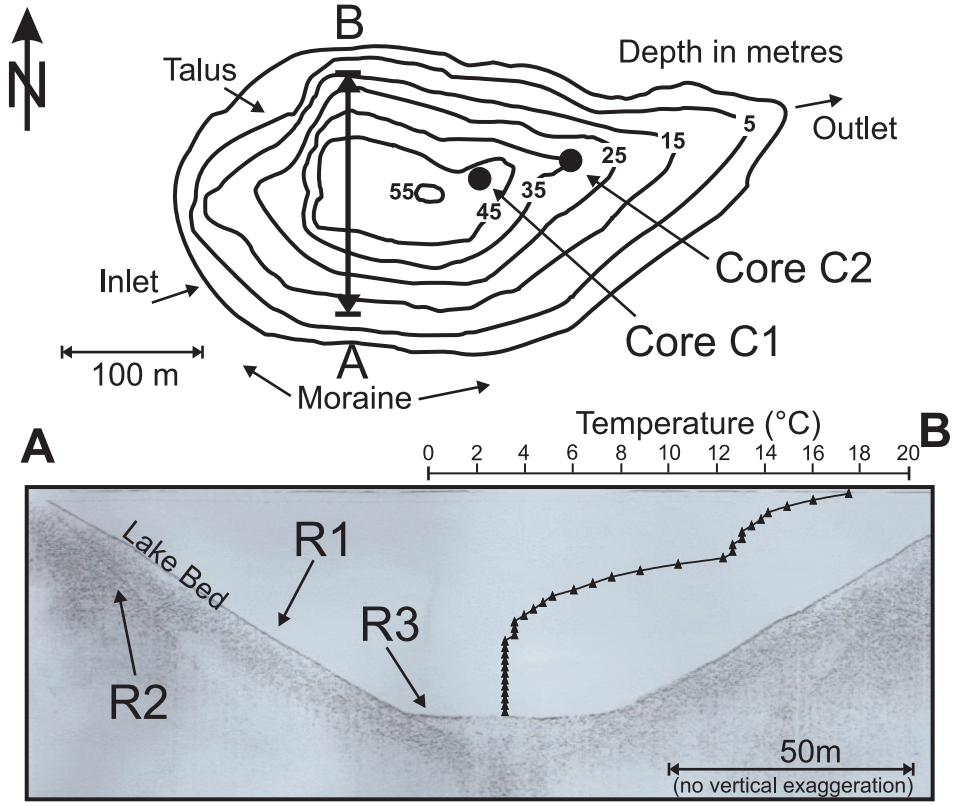


Little Ice Age moraine was deposited upstream of this older moraine; only hummocky terrain, comprised of glacial diamict, was seen.

Otokomi Lake has a surface area of about 10 ha and a Secchi depth of 5.9 m. The results of the sonar survey show the lake to have a symmetric funnel-shaped profile with a radius of 105 m, basin slopes of ~30°, and a maximum depth of 54 m. The lake exhibits thermally stratified water in the summer months, with a thermocline depth of ~14 m (Fig. 3).

A percussion coring system described by Reasoner (1986) was used to collect two cores from Otokomi Lake in the early spring of 2001. The two core locations were chosen on the assumption that the lake bed had a symmetrical basin profile, making core sites along the lake's long axis near the basin center good candidates for maximum sediment recovery. Thus, core C1 was taken from the center of the lake, and core C2 was taken about 100 m east of core C1 towards the lake's outlet. Upon retrieval from the lake bottom, the cores were sectioned into ~50 cm lengths for transport to the University of Calgary, Calgary, Alberta, where they were stored frozen for future analysis.

## Laboratory analyses

While frozen, the core sections were X-rayed at a voltage of 110 kV and amperage of 10 MA, for 2 min at a distance of 170 cm from the X-ray source. The resultant film was then scanned into a computer so that gray-scale values along the length of each core, which are correlative with sediment density (Bresson and Moran 1998), could be determined and plotted. Next, a circular saw equipped with a diamond blade was used to split the frozen cores lengthwise. The slag from the sawing process was cleaned from the cut surfaces before the cores were digitally photographed at high-resolution. The split core sections were then allowed to thaw for 1 day before sedimentary structures, colours, textures, and macrofossil locations were recorded in a detailed log. A modified syringe capable of extracting 1 $cm^3$ plugs of sediment was used for the majority of the core sampling; however, the analysis of the core's coarse (>1 mm) grain fraction involved the horizontal partitioning of core sediment into 1 cm thick semicircular slices having a volume of about 82 $cm^3$.

Three distinct light gray, fine-sand sedimentary units were suspected of containing tephra. The presence of glass shards in each unit was confirmed through binocular-microscopic inspection of air-dried samples. A mixture of Calgon and Decalin (specific gravity = 2.42) was then used to separate the glass fraction from the heavier minerals in each sample. Chemical analyses and backscattered electron images of the glass fraction of each sample were obtained at the University of Calgary using a JEOL JXA-8200 electron microprobe.

Total organic and total inorganic carbon percentages were determined by combusting 1 $cm^3$ sediment samples at 550 and 950 °C, respectively. The sample size and LOI (loss on ignition) time recommendations of Heiri et al. (2001) were followed to ensure reproducibility and accuracy. Ignition times

© 2006 NRC Canada

were 4 h for the organic carbon analysis and 2 h for the inorganic carbon analysis.

The fine-grain (≤1 mm) sediment fraction from the cores was using a laser-scattering particle analyzer. Preparation of the air-dry samples, with a requisite weight between 0.15 and 0.2 g, involved the addition of 2 mL of 30% hydrogen peroxide to digest organic material, followed by the addition of 10 mL of a 2.5% Calgon solution to deflocculate clay material. The coarse-grain (>1 mm) fraction of the core sediment was obtained through a wet-sieve analysis. Pre-weighed, oven-dry sediment slices were wet sieved at a mesh size of 1 mm before being re-dried and re-weighed. No hydrogen peroxide digestion was performed during the coarse-grain analysis because of the highly inorganic nature of the sediment, as determined by the LOI data.

Magnetic susceptibility (MS) (in SI units) measurements were performed along the length of each core subsection at 5 mm intervals using a hand-held Exploranium KT-9 Kappameter, equipped with a 10 kHz oscillator. To increase accuracy, 30 readings were taken at each point and then averaged prior to analysis.

## Results

### Descriptive stratigraphy

Just over 240 cm of sediment were retrieved from the bottom of Otokomi Lake in core C1, whereas C2 contained about 120 cm of sediment upon recovery. In addition to the sedimentary structures unique to each core, there were three very similar sedimentary units visually identified in both cores at comparable depths. These units included a suspected volcanic ash unit, a pebble-rich zone, and a well-demarcated thin pebble-rich horizon. Based on this observation it was concluded that the longer core C1 likely contained a more complete sedimentary record than C2. For this reason, the problem of moraine emplacement was addressed primarily using the analyses conducted on core C1.

During the retrieval of C1, many coarse pebbles in a clay-rich matrix were observed adhering to the inside of the core barrel below the core catcher. This material fell from the core tube during handling and was not retained for analysis, although it may have represented the basal till layer over which the lake sediment settled.

The dominant sediment colour in the remainder of C1 ranged from pink to shades of brown and red. Above the core catcher to a depth of 205 cm in C1, there was a zone of laminated clay-rich sediment with scant pebbles. Directly above this zone, centered at depths of 204.2 and 200.9 cm, were two suspected volcanic ash layers with thicknesses of 4 and 10 mm, respectively. Above these layers the core changed dramatically to a dark brown, silty clay matrix with an abundance of scattered pebbles. At a depth of 170 cm, the core matrix changed to light red, silty clay, with the abundance of scattered pebbles remaining. This silty clay matrix was interrupted at 124 cm by a 15 cm thick zone of clast-supported coarse pebbles containing a matrix of suspected volcanic ash. Directly above this zone was a 10 cm thick globular lens of suspected volcanic ash, centered at 103.4 cm. The light red, silty clay matrix with many scattered pebbles resumed above this lens to a depth of 86 cm, above which the matrix colour changed to dark red. This dark red sediment was overlain by a 5 cm thick layer of organic-rich sediment at the top of the core.

C1 contained four silt-dominated horizons, one clay-rich horizon, and over 30 conspicuous pebble-dominated minerogenic horizons, ranging in thickness from a few millimetres to several centimetres. The pebbles in the coarse horizons were matrix supported, often oriented parallel to bedding, and appeared to be the basal portions of graded beds. With the exception of one thin pebble layer at 221 cm, all of the coarse minerogenic horizons in C1 were found above 185 cm within the silty clay pebble-rich matrix (Fig. 4).

### X-radiography

The gray-scale values of the C1 X-ray image were generally found to decrease with depth. Almost all sample points from the top of the core to a depth of 40 cm had a gray-scale value of 200, which was the highest value recorded for the entire core. The two main zones, where the general gray-scale trend was interrupted, were between the depths of 107 and 124 cm and at 183 cm. The 107–124 cm zone represents a "spike" of low gray-scale values, whereas the 183 cm mark represents a depth above which the gray-scale values drop suddenly before continuing to increase upward (Fig. 4).

### Loss-on-ignition analysis

Organic carbon values in Otokomi Lake C1 ranged from 1.5% to 12.3% by weight. From the bottom of the core to a depth of 126 cm, organic carbon values remained close to 3%; above this depth, values generally increased but displayed more variability. Inorganic carbon values in C1 ranged from 0% to 3.6% by weight. Loss-on-ignition values were the highest at the top and bottom of the core, with the lowest LOI values occurring between depths of 78 and 151 cm (Fig. 4). No combustion data were generated for the 97–124 cm interval because of the extremely coarse nature of the sediment.

### Grain-size analysis

The percentage of clay in C1 ranged from 0% to 33.4%, with the highest clay percentages near the core bottom. Clay percentages were near zero over the interval of 118–92 cm and also from 54 cm to the core top. The silt content in C1 ranged from 10% to 97%, with the highest silt values near the top and bottom of the core and relatively lower silt values over the interval of 40–190 cm. The percentage of sand in C1 ranged from 5.5% to 89%. In contrast to the silt content values, the sand values were low near the top and bottom of the core and relatively higher over the interval of 35–202 cm. The coarse (>1 mm) fraction of the sediment in C1 ranged between 1.3% and 83% by weight. Values were low near the top and bottom of the core and were relatively higher over the interval of 67–183 cm, with the highest percentage of coarse material found near the depth of 115 cm (Fig. 4).

### Magnetic susceptibility

The MS values for core C1 ranged from $0.01–1.82 \times 10^{-5}$ SI units, with a general trend of MS increasing with depth. During the measurement process, the MS values predictably dropped as the instrument neared the end of each core subsection. It is presumed that these "edge effects" were the cause of the low MS values at these six depths, rather than

© 2006 NRC Canada

**Fig. 4.** Descriptive stratigraphy for percussion cores C1 and C2 along with laboratory analyses for percussion core C1. The stratigraphic location of visible organic fragments, pebble horizons and (or) zones, silt and clay horizons, and possible stratigraphic correlations between C1 and C2 are indicated. The locations of the three suspected volcanic ash units are indicated beside C1. M, Mazama ash; GP, Glacier Peak G ash; SH, Mt. St. Helens Jy ash. Laboratory analyses include X-ray gray-scale values, loss on ignition at 550 °C and 950 °C, and grain-size analyses separated into wt.% of grains > 1 mm, as well as relative percentages of sand, silt, and clay. A dashed line demarcates 185 cm in depth, above which a visible coarsening of grain size was seen in C1. Mag., Magnetic.

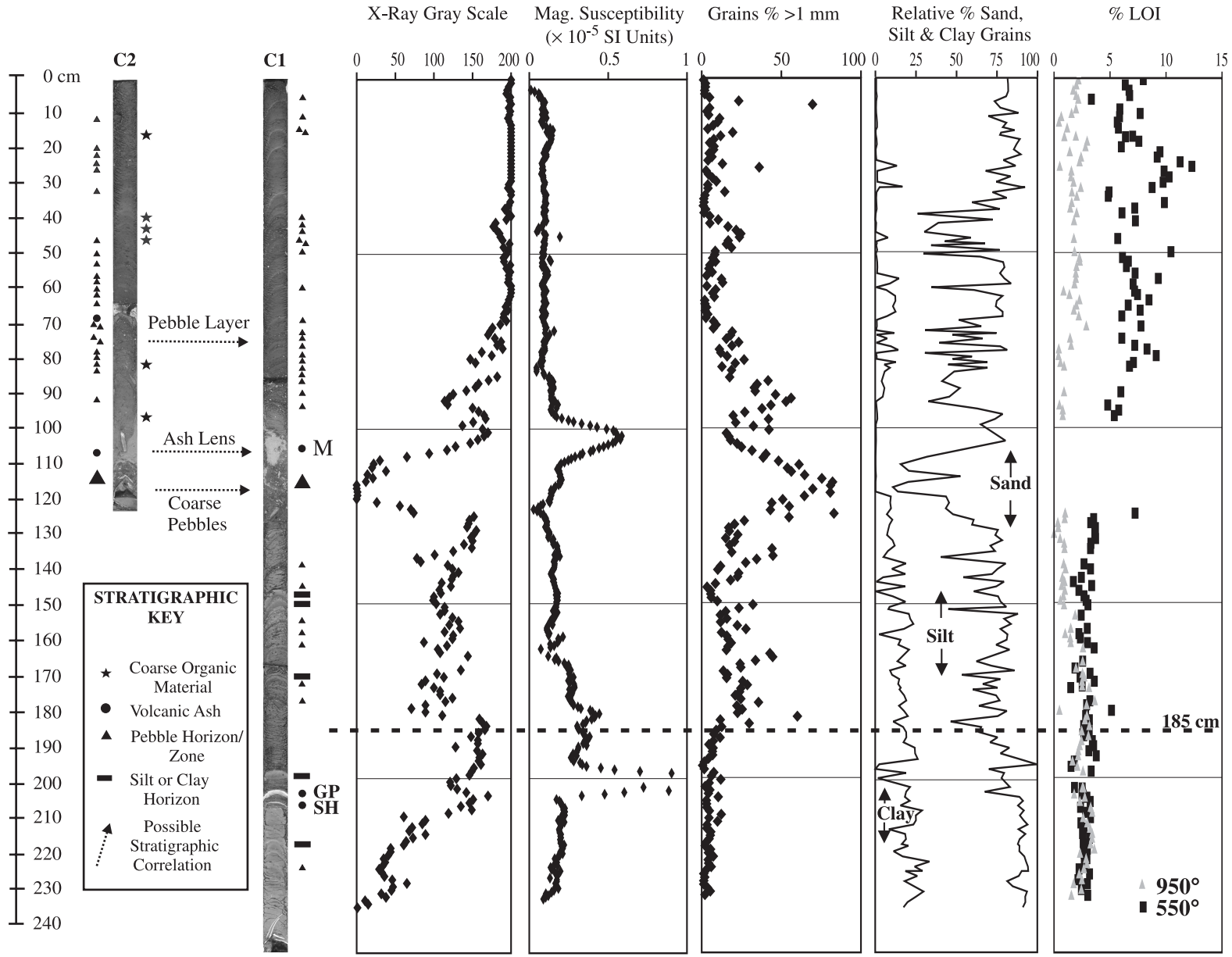




© 2006 NRC Canada

the nature of the sediment itself. There were also three zones where MS values deviated positively from the overall trend. The MS peaks centered at 201 and 102 cm, which corresponded to depths where the suspected volcanic ash layers were identified. The third and smallest MS peak was centered at 181 cm (Fig. 4).

### Tephra identification

All three of the suspected volcanic ash layers in C1 consisted of grains ranging in size from silt to fine sand, displayed very high MS (Fig. 4), and displayed vitreous shards when analyzed under a binocular microscope at ×100 magnification. Under ×10 magnification, the upper and lower boundaries of the 200.9 and 204.2 cm layers appeared sharply defined and were laterally continuous to the edge of the core tube. The lens that was centered at 103.7 cm was laterally discontinuous and had convoluted upper and lower contacts. The 204.2 cm layer appeared off-white, whereas the layer that was centered at 200.9 cm had a banded appearance with alternating off-white and black bands, giving it a "salt and pepper" look. The layer centered at 103.7 cm had a gray appearance, with no banding.

The scanning electron microscopy images of the light fraction of each ash layer revealed many vitreous, vesicular shards. The shards in each sample appeared platy and included elongate, furrowed, Y-shaped, curved and more complex varieties. The glass shards also contained phenocrysts, which differed from the glass in their geometry, brightness, and lack of vesicles. The vesiclularity of the three glass samples differed; the layer centered at 204.2 cm contained the most vesicles, followed by the layer centered at 200.9 cm, and lastly by the ash lens centered at 103.7 cm. The shards from the ash layer centered at 200.9 cm were, on average, the largest of the three samples, with the other two samples having shards of about the same size. The 103.7 cm sample contained shards of two distinct photographic tones and chemistries (Fig. 5). One-third of the shards in the 103.7 cm sample had a light tone and contained relatively more CaO, FeO, $TiO_2$, MnO, $Al_2O_3$, and MgO, whereas the darker grains in the sample were enriched in $SiO_2$, $Na_2O$, and $K_2O$ (Table 1). Of the three ash layers, the 200.9 and 204.2 cm ash samples had chemically very similar glass fractions, whereas both fractions of the 103.7 cm sample were chemically more distinct (Table 1).

## Discussion

### Mechanisms of sedimentation in Otokomi Lake

Otokomi Lake can be characterized as a dimictic, oligotrophic alpine lake. A measured Secchi-disc transparency of 5.9 m indicates low levels of lake productivity at present (Håkanson and Jansson 1983). Otokomi Lake appears to have been unproductive throughout much of its past as well; almost every sample analyzed by LOI had < 10% organic carbon by weight.

With a relatively shallow thermocline and a deep basin profile, Otokomi Lake likely experiences little resuspension of fine particulate matter during turnover events (Larsen and MacDonald 1993). However, because the thermocline represents a boundary between low- and high-density water masses, suspended particulates entering the lake may be dispersed throughout the basin along this boundary. The thermocline may be an important distribution mechanism during periods of prolonged ice cover or drought when incoming water volumes and sediment loads are low.

The small surface area of Otokomi Lake provides little fetch for the generation of large waves. In addition, the steep basin morphology, coupled with a narrow shoreline, allows only a small portion of the nearshore zone to be disturbed by wave action. Therefore, the resuspension and redistribution of sediment through wave processes is thought to play a minimal role in the sedimentation dynamics of Otokomi Lake.

The dominant mechanism for introducing clastic sediment into Otokomi Lake appears to be overland transport, including fluvial and mass-movement processes. For example, the bathymetric map of Otokomi Lake shows the effect of the nearby talus slope on basin morphology; a shelf can be seen building into the lake's northwest corner. With a large portion of the sediment slopes in the lake basin dipping at an angle near 30°, periodic sub-aqueous slumping is also expected in areas where incoming sediment loads cause slope loading and oversteepening.

Snow avalanches are expected to occur commonly on the steep slopes above the lake. For snow avalanches to deliver sediment into Otokomi Lake, however, they must reach the lake itself. Judging from the statistical "runout ratio" method employed by Nixon and McClung (1993), avalanches originating south and northwest of Otokomi Lake commonly reach the lake. Therefore, any clastic sediment entrained within the avalanche debris on the lake surface would enter the lake during the spring melt. The ability of snow avalanches, particularly wet-snow avalanches, to erode the ground surface and incorporate clastic material into their deposits has been documented (Luckman 1975; Gardner 1983). Ice-rafting processes, as described by Smith (2000) and Luckman (1975), are also capable of transporting coarse sediment from the high-energy shoreline environment to the centers of lake basins.

### The sedimentary record

One of the most clearly identifiable characteristics of the percussion cores collected from Otokomi Lake was the amount of coarse clastic sediment within them, indicating the ability of high-energy sediment transport mechanisms to affect even the basin deeps. Based on calculations using the Manning equation, high-energy stream inputs are capable of transporting pebbles to Otokomi Lake; however, the flow expansion that would occur as these streams enter Otokomi Lake limits the ability of their bedload to reach the basin center, where C1 was collected. Ice rafting may explain the scattering of matrix-supported pebbles seen above 185 cm in C1, but not the graded pebble beds found elsewhere, owing to its nature as a selective transport mechanism favouring coarse shoreline sediment. Sub-aqueous slumping events along the 30° sediment slopes and sediment-laden snow avalanches then appear to be the only mechanisms capable of depositing the graded pebble beds found in the core. The 15 cm thick zone of clast-supported pebbles at 124 cm in C1 is interpreted to be a massive snow avalanche deposit. The paucity of silt and clay in the deposit and its presence in both percussion cores are the result of a high-energy transport mechanism, such as

© 2006 NRC Canada

**Fig. 5.** A comparison of the relative abundance of FeO, CaO, and $K_2O$ in the three volcanic glass samples analyzed in this project with accepted relative abundances for some widespread western North America tephra layers. Squares represent the 103.7 cm ash sample, with analyses for the dark (D), light (L) and dark + light (D+L) grains included. The circle represents the 200.9 cm layer and the star represents the 204.2 cm layer. M, Mazama; GP, Glacier Peak set G; SH, Mt. St. Helens; BR, Bridge River; P, Pearlette; BT, Bishop Tuff. All comparative data obtained from Westgate and Gorton (1981) except the St. Helens Jy data, which was obtained from Carrara (1989). The scanning electron microscopy images show the shard morphology and photographic tone of the three ash units.

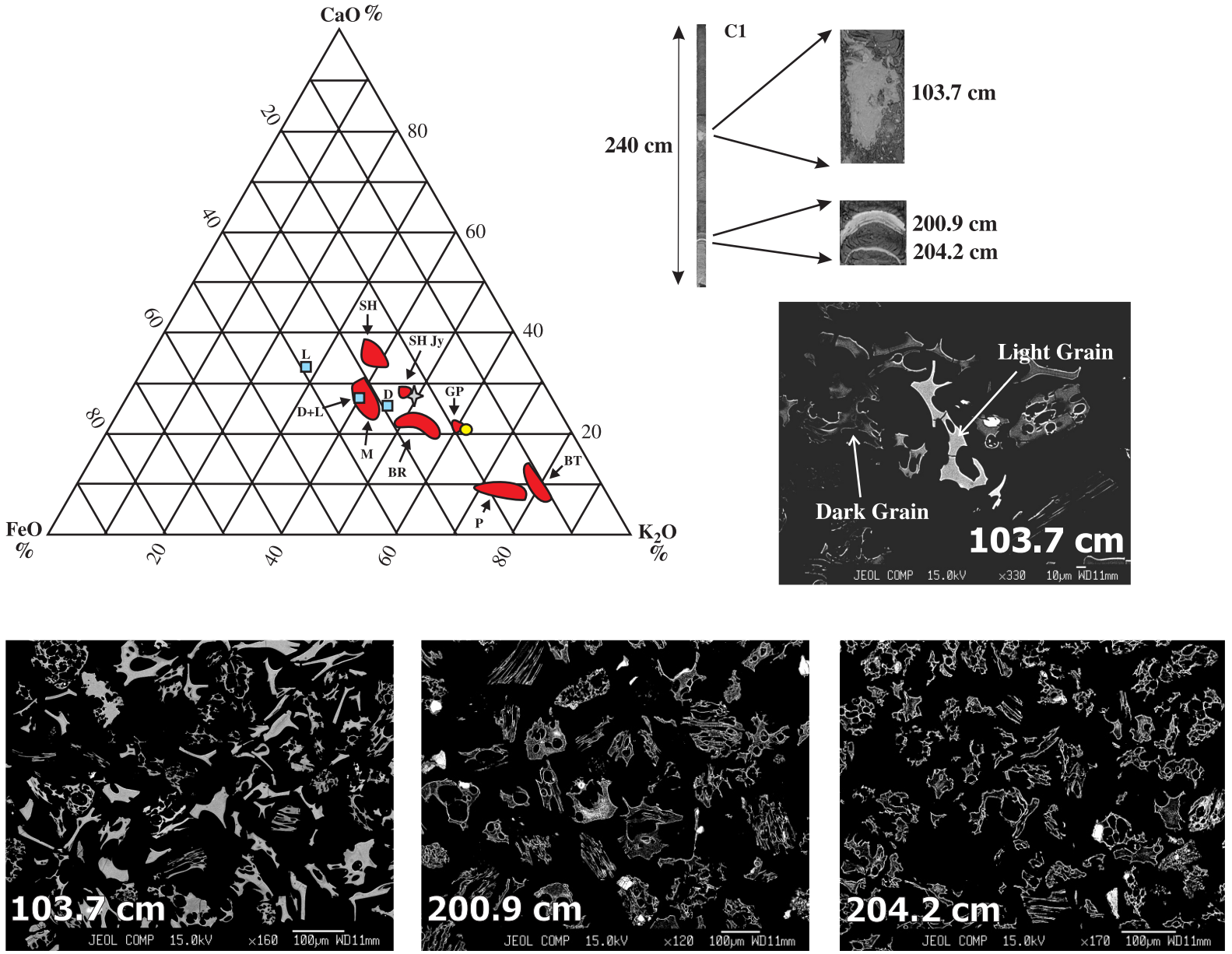


© 2006 NRC Canada

**Table 1.** Average chemical composition of the three volcanic glass samples collected from Otokomi Lake C1.

| | $K_2O$ (%) | CaO (%) | *FeO (%) | $Na_2O$ (%) | $SiO_2$ (%) | $TiO_2$ (%) | MnO (%) | $Al_2O_3$ (%) | MgO (%) | Total (%) | *n* |
|---|---|---|---|---|---|---|---|---|---|---|---|
| 103.7 cm (all grains) | 2.69 | 1.90 | 2.24 | 5.27 | 71.76 | 0.50 | 0.06 | 14.95 | 0.62 | 100.00 | 49 |
| 103.7 cm (dark grains) | 2.82 | 1.58 | 1.86 | 5.33 | 72.88 | 0.43 | 0.05 | 14.58 | 0.47 | 100.00 | 36 |
| 103.7 cm (light grains) | 2.34 | 2.81 | 3.29 | 5.12 | 68.67 | 0.69 | 0.07 | 15.96 | 1.05 | 100.00 | 13 |
| 200.9 cm | 3.55 | 1.16 | 0.97 | 3.93 | 77.22 | 0.19 | 0.03 | 12.71 | 0.23 | 100.00 | 56 |
| 204.2 cm | 2.49 | 1.35 | 1.17 | 3.92 | 77.21 | 0.18 | 0.02 | 13.37 | 0.27 | 100.00 | 46 |

**Note:** All values corrected to a total of 100%. Original totals ranged from 94.1% to 97.5%, with the remaining fraction assumed to be water. The number of sample points (*n*) used in each analysis is presented in the last column. * indicates total iron expressed as FeO.

a snow avalanche, that is capable of selectively transporting coarse material over a broad area.

A congruency can be seen between the sand data (>0.063 μm) in the fine-grain analysis and the data from the coarse-grain (>1 mm) sieve analyses. With the exception of slightly more scatter in the sand data, the coarse-grain data trends mimic those of the sand data. Both show relative increases and decreases at the same depths and of similar magnitudes. The silt data set, on the other hand, is the mirror image of the sand and coarse-grained data sets. The silt data set shows relative increases at depths where the two coarser data sets show relative decreases and vice versa. A possible explanation for the positive relationship between the sand and coarse-grain data sets would be that the same mechanisms that are transporting and distributing the coarse (>1 mm) material within the basin are also responsible for the transport and distribution of the sand-sized grains. When these processes are more active, whether they be ice rafting, snow avalanching, basin slumping, or extra-basinal mass movement events, the sedimentary record is biased towards grains sand-sized and larger. When these processes are not as active, the slower processes of fine-grain sedimentation dominate, characterized by silt and clay deposition.

The variations in clay concentration throughout C1 may relate to changes in clay availability in the sediment source areas. Following Wisconsinan deglaciation, the veneer of exposed glacial till in Rose Basin would have been an ample source of clay. This availability would have diminished as the clay was slowly washed from the till over time and also as the till became covered with pioneering plant species. This is evident in the clay data from C1, where percentages are highest at the bottom of the core and steadily drop to almost 0% at the top of the core.

## Core chronology and sedimentation rates

Three prominent late Quaternary ash deposits have been identified in northwestern Montana. The youngest of the three is the Mazama ash (ca. 6730 BP), which is underlain by a Glacier Peak G (ca. 11 200 BP) – Mt. St. Helens Jy (ca. 11 400 BP) ash couplet (Lemke at al. 1975; Carrara 1989; Franklin et al. 1993). Traditionally, differentiating these three ash layers has been based on chemical analyses of the glass shards. Each ash layer identified in this study has a glass chemistry that correlates well with one of the three ash layers mentioned earlier in the text (Fig. 5). The thick lens of ash centered at 103.7 cm in C1 is chemically similar to Mazama ash, the 200.9 cm layer is chemically similar to Glacier Peak G ash, and the 204.2 cm layer is chemically similar to Mt. St. Helens Jy ash. In addition to their glass chemistry, the three ash layers in this study have the same relative stratigraphic position, thickness, and texture as the late Quaternary ashes mentioned earlier in the text (Lemke et al. 1975; Osborn 1985; Carrara 1989; Carrara and Trimble 1992). The occurrence of two chemically distinct glass fractions in the Mazama ash was first recognized by McBirney (1968) from samples collected adjacent to the volcano itself. The two glass fractions are thought to represent closely spaced eruptions from two chemically distinct magma pools. The two distinct glass species would presumably be present throughout the known fallout range of the Mazama ash, or at least at sites closer to the ash source than Otokomi Lake; however, partitioning of the Mazama ash into two chemically distinct glass species is only found in McBirney's (1968) data. Therefore, in this study, the Mazama ash analysis in which the two glass fractions are grouped together is used as the comparator. Based on agreement between the chemical and stratigraphic data of this study and that of the literature, the three ash units in C1 are interpreted to be Mazama (103.7 cm), Glacier Peak G (200.9 cm), and Mt. St. Helens Jy (204.2 cm). Although the volcanic ash identified in C2 was not chemically analyzed with the microprobe, its texture, volume, and approximate stratigraphic position were consistent with those of the Mazama ash.

In both C1 and C2, the globular appearance of the Mazama ash indicated that it may have migrated up-core from its original stratigraphic position. In C1, the bulk of the laterally discontinuous Mazama ash lens was centered at 103.7 cm. This lens was vertically continuous with ash that was intermixed with the underlying avalanche debris, having a lower boundary within the debris at 114 cm. Sediment liquefaction, initiated by core-barrel vibration during the collection process, and the close association of the ash with high-energy avalanche debris may both be reasons why the ash appeared to be displaced from its original stratigraphic position. The two lower ash units, however, did not appear to have migrated from their original stratigraphic positions. Although they were only present in C1, their lateral continuity, conformable contacts, characteristic thicknesses, and relative stratigraphic positions and textures were all reasons that the lower two ash units were used as chronologic markers for core C1.

Very few organic fragments were found in C1 or C2 that were large enough for accelerator mass spectrometry radiocarbon dating. The few that were found were either recovered from very high stratigraphic levels or closely associated with the 15 cm thick zone of avalanche debris in C1 and C2, therefore limiting their ability to serve as accurate chronologic

© 2006 NRC Canada

controls for moraine emplacement. For these reasons, the chronology of the Otokomi sediment cores is based on the identified ash units.

Prior to calculating sedimentation rates, there was a need to determine the depth and thickness of all horizons that were deposited instantaneously. These horizons represent zero time in a stratigraphic sense and, therefore, serve to over-represent sedimentation rates. The "equivalent" depth at any given point was then calculated by subtracting the total thickness of overlying sediment that was deposited instantaneously. This correction process was limited by the difficulty of accurately identifying and interpreting intervals of instantaneous deposition; because of the extremely coarse nature of C1, periods of rapid deposition that produced thin layers, or layers of intermediate grain size, may have been overlooked. This type of error would have resulted in an overestimation of sedimentation rates. Using this correction procedure, the Mt. St. Helens Jy ash layer had an equivalent depth of 144.4 cm. If the rate of sedimentation for the overlying material was constant, it would be equivalent to 0.0132 cm/a. To test the accuracy of this sedimentation rate estimation, the appropriate depth for Mazama ash (6845 BP) in C1 was calculated. With a sedimentation rate of 0.0132 cm/a, the predicted depth for Mazama ash in C1 would be 87 cm. This depth was consistent with stratigraphic observations of C1, where the equivalent depth for Mazama ash was 84 cm (corresponding to an observed depth of 103.7 cm). The general agreement between these two depth estimates serves as additional evidence to support the use of the volcanic ash units as time stratigraphic markers for C1. The 3 cm difference between the estimated and equivalent depths for Mazama ash in C1 may be attributed to errors associated with the depth correction technique or to natural sedimentation rate variations that may have occurred over the stratigraphic interval in question.

The presence of about 35 cm of sediment below the Mt. St. Helens Jy ash suggests that deglaciation of Rose Basin significantly predated 11 400 BP. Using the previously calculated sedimentation rate of 0.0132 cm/a, the bottom of C1 (240 cm) corresponds to an age of about 14 100 BP. Although there is no glacial diamict plug at the bottom of C1, coarse pebbles were discovered on the inside of the core barrel, below the core catcher, at the time of recovery. If this material, which likely impeded further core penetration into the lake sediment, represents the basal till layer in Otokomi Lake, then 14 100 BP is a reasonable time estimate for the initial deglaciation of Rose Basin. Other cores collected from more productive alpine lake basins in the North American Cordillera have encountered basal till at depths between 250 and 310 cm (Spooner et al. 1997, 2002; Mazzucchi et al. 2003; Reasoner et al. 1994). Therefore, it seems possible that the basal till layer in such an unproductive alpine lake could be found below 240 cm of sediment. The basal age of 14 100 BP for Otokomi Lake, however, may actually be a "minimum" estimate. Fine-grain sedimentation rates during the early stages of lake development are often lower than the rates at higher stratigraphic levels (Fergusson and Hills 1985; Reasoner et al. 1994; Gerloff et al. 1995). Therefore, the sedimentation rate below 204 cm in C1 may have been lower than the 0.0132 cm/a rate calculated from higher stratigraphic levels; however, a basal age of ≥14 100 BP is significantly older than some of the oldest estimates for deglaciation in the North American Rockies. Fergusson and Osborn (1981) dated snail shells from post-glacial sediments in Elk Valley, British Columbia, at ca. 13 430 BP. Kearney and Luckman (1987) reported an age of ca 13 500 BP for organic material at the bottom of Maligne Lake in Jasper National Park. Fulton (1984) suggested that retreat of the Cordilleran Ice Sheet was underway by 13 000 BP. This discrepancy could be explained if the post-glacial sedimentation rates in Otokomi Lake were in fact quite high; however, this explanation contradicts the low post-glacial sedimentation rates predicted by Fergusson and Hills (1985) and others. If, on the other hand, the ≥14 100 BP estimate for deglaciation in Rose Basin is appropriate, it may be related to the relatively low latitude of Glacier National Park relative to many of the sites described in the previous text, or the proximity of Rose Basin to the eastern margin of the mountain ice fields that covered the park (Carrara 1989). These factors would have contributed to a relatively early deglaciation in the Glacier National Park region and the consequent exposure of Rose Basin early in the process.

The notion that the clay-rich sediment at the bottom of C1 represents the early stages of sedimentation in Otokomi Lake is corroborated by the LOI data and observations made during wet sieving. During the wet-sieving portion of the coarse (>1 mm) grain analysis, only three organic fragments were recovered over the 200–240 cm interval, whereas 137 organic fragments were recovered from the top 40 cm of the core. The lack of organic fragments in the bottom 40 cm of C1 reflects the absence of plant species in Rose Basin during that time of sediment deposition. In addition, the 550 °C LOI values are at their lowest over the 204–240 cm interval, reflecting the low levels of lake productivity expected in a recently deglaciated alpine lake.

**Evidence of moraine deposition**

Assuming that C1 contains nearly the entire post-glacial sedimentary record of Otokomi Lake, the sedimentary signature related to the emplacement of the Crowfoot moraine should be present at some level in the core. This signature should be one associated with cold conditions, and would presumably have a texture resulting from the sedimentary effects of sudden moraine emplacement along the lake's south shore.

Many of the data sets generated from the sedimentary analysis of C1 show a distinct change above 185 cm (Fig. 4). This deviation it is consistent across the data sets and appears to indicate sedimentary change associated with glacial advance and moraine emplacement.

Going up-core, the weight percent of coarse material in C1 jumps ~15% at 185 cm; this quantifies the visible coarsening that was apparent above this depth. Because higher sediment densities are related to low X-ray gray-scale values, the general decrease in gray scale with depth in C1 is consistent with the expectation of higher bulk densities at lower stratigraphic levels (Last and Smol 2001). The sudden decrease in gray-scale values above 185 cm opposes this general trend and represents a sudden increase in the sediment density above that depth. Because lithified rock fragments generally have a higher density than unconsolidated sediment, an increase in the percentage of rock fragments would likely in-

© 2006 NRC Canada

crease the average sediment density at a given depth. Therefore, the observed deviation in the X-ray data can be also attributed to the increased density of coarse rock fragments above 185 cm. Similar to X-ray data, MS data can also be thought of as a proxy for sediment density (Thompson et al. 1975). The increase in MS values above 185 cm is therefore attributed to the sediment density increase already established from the previous data sets. As with the X-ray data, the general up-core decrease in MS is likely a result of the increasing organic and water content of the sediment.

Moraine deposition adjacent to the lake can be used to explain the increased density of coarse rock fragments in C1 above 185 cm. The appearance of a 200 m long and 10 m high mound of unconsolidated glacial till along the shore of Otokomi Lake would likely intensify the majority of the coarse sediment transportation and deposition mechanisms acting within the basin, with the exception of snow avalanches. Once in place, small mass-movement events or stream activity could have easily moved coarse sediment from the flank of the moraine to the nearshore environment of the lake. Ice rafting and subaqueous slumping along the 30° sediment slopes could then have transported this coarse material to the basin center. Inorganic sediment, commonly characterized by having a relatively coarse grain size, also has been attributed to upstream glacial activity (Engstrom et al. 1990; Reasoner et al. 1994; Menounos and Reasoner 1997).

Warming of lake water is commonly associated with increased calcium carbonate precipitation (Håkanson and Jansson 1983), which causes an enrichment of the inorganic carbon content of associated sediments. In this study, the inorganic carbon data set shows an interesting up-core trend whereby inorganic carbon increases up-core below 200 cm, decreases up-core to a depth of 194 cm and then increases up to, and above, the 185 cm depth previously associated with up-core sediment coarsening. These parallel trends may represent initial post-glacial warming in Glacier National Park, which was interrupted by a cooling event and resumed warming shortly thereafter. These data would put the height of the cooling at 194 cm, at which depth the inorganic carbon values are low. It is important to note that the cooling associated with this depth is not necessarily inconsistent with the coarse sediment influx into the Otokomi Lake occurring above 185 cm. Although the cool conditions needed for glacial activity and moraine deposition may have existed at the time the sediment at 194 cm were deposited, the environmental conditions necessary for mobilizing the moraine sediment may not have existed. The warming trend that followed the cooling event at 194 cm may have created the ice-free conditions necessary for effective transport of moraine sediment into the lake. Once these coarse clastic sediments began entering the lake, more time would have been required for the associated processes of ice rafting and basin slumping to become accelerated. This time lag may explain the 9 cm offset between sediment that is associated with the cooling event and sediment that first records coarse influx into the basin. Based on the approximate 0.0132 cm/a sedimentation rate, the cooling event at 194 cm responsible for moraine deposition would have occurred at 10 590 BP. This age is within the established range for Younger Dryas cooling.

If, however, the sedimentary trends in the lower portion of C1 are not associated with climatic cooling and subsequent moraine deposition, then several issues must be addressed. If moraine emplacement happened before 10 590 BP, there is no discernable record of its effect on lake sedimentation. Presumably the initial post-glacial warming experienced in Rose Basin before 10 590 BP would have mobilized till if a moraine were present at that time. Instead, clay-rich silty sediment was deposited in Otokomi Lake up to the 185 cm depth, which indicates a lack of coarse sediment availability. Conversely, if moraine deposition postdates the coarsening at 185 cm, then another mechanism must be evoked to explain the coarsening. An increase in avalanche frequency above 185 cm is not a likely explanation when considering the environment of deposition of the sediment below 185 cm in C1. The cold, sparsely vegetated, recently deglaciated landscape, which would have been present during the deposition of the lowermost sediment in C1, would likely have favored avalanche activity; however, because very little coarse material occurs in this lower portion of the core, the avalanche frequency within the basin does not appear to be correlated with coarse sediment influx into Otokomi Lake. In addition, there do not appear to be any other obvious sedimentary changes in C1 between the 185 cm depth and the Mazama tephra lens that are easily related to post-10 590 BP moraine deposition and climatic cooling. Although this observation does not preclude the possibility that moraine deposition could have occurred without leaving a recognizable sedimentary signature in Otokomi Lake, the fact that the 185 cm coarsening in C1 is most easily explained by mechanisms associated with moraine deposition and subsequent coarse sediment mobility appears to support Younger Dryas cooling in Rose Basin.

## Conclusions

Sedimentation in Otokomi Lake is characterized by both low-energy and high-energy transport and distribution mechanisms. Low-energy mechanisms, likely associated with low-flow fluvial inputs, are responsible for depositing clay and silt within the lake basin. High-energy mechanisms, such as sub-aqueous mass movements along oversteepened portions of the lakebed, ice rafting and drainage basin mass-movements, are responsible for depositing sand- to pebble-sized clasts within the lake basin.

Based on the chronological control offered by three volcanic ash layers in C1, deglaciation of Rose Basin has a minimum bracketing age of 11 400 BP, although 14 100 BP is the estimated basal age for the core. The 14 100 BP basal age estimate for Otokomi Lake indicates that deglaciation for this portion of western North America may have been significantly earlier than previous estimates.

Correlative shifts in the LOI, coarse (>1 mm) grain size, MS, and X-ray gray-scale data for C1 were all related to a sedimentary change in Otokomi Lake brought about by the emplacement of the adjacent Crowfoot moraine. The estimated emplacement date for the Crowfoot moraine is 10 590 BP, which is within the Younger Dryas interval. This age estimate supports the hypothesis that Crowfoot moraines represent a regional response in western North America to Younger Dryas cooling.

© 2006 NRC Canada

## Acknowledgments

Funding for this research was provided by G. Osborn's Natural Sciences and Engineering Research Council (NSERC) operating grant, as well as an NSERC PGSA scholarship and an Informatics Circle of Research Excellence graduate scholarship, both awarded to M. MacLeod. E. Lynn, D. Diaz, and M. Hupman were field assistants during the summer of 2001. D. Mazzucchi, E. Lynn, and T. Mang aided with the collection of the percussion cores in April 2001. R. Marr was of great help with microprobe data interpretations. Thanks also to the technical staff at the University of Calgary: L. Bloom, B. Mottle, M. Smith, and D. Glatiotis. Thanks to the staff of Glacier National Park for allowing this project to be conducted, including the accommodating staff at the West Glacier Science Center, as well as J. Fowler, L. Marnell, D. Jacobs, and the helpful trail crew.

## References

Alden, W.C. 1953. Physiography and glacial geology of western Montana and adjacent areas. US Geological Survey, Professional Paper 231.

Alley, R.B., Meese, D.A., Shuman, C.A., Gow, A.J., Taylor, K.C., Grootes P.M. et al. 1993. Abrupt increase in Greenland snow accumulation at the end of the Younger Dryas event. Nature, **362**: 527–529.

Alley, R., Mayewski, P., Sowers, T., Stiuver, M., Taylor, K., and Clark, P. 1997. Holocene climate instability: a prominent widespread event 8200 yr ago. Geology, **25**: 483–486.

Barnosky, C.W. 1989. Postglacial vegetation and climate in the northwestern Great Plains of Montana. Quaternary Research, **31**: 57–73.

Beget, J.E. 1983. Radiocarbon-dated evidence of worldwide early Holocene climate change. Geology, **11**: 389–393.

Bennett, K.D., Haberle, S.A., and Lumley, S.H. 2000. The last glacial-Holocene transition in southern Chile. Science, **290**: 325–328.

Bresson, L.M., and Moran, C.J. 1998. High-resolution bulk density images, using calibrated X-ray radiography of impregnated soil slices. Soil Science Society of America Journal, **62**: 299–305.

Broecker, W.S., Kennett, J.P., Flower, B.P., Teller, J.T., Trumbore, S., Bonani, G.et al. 1989. Routing of meltwater from the Laurentide ice sheet during the Younger Dryas cold episode. Nature, **341**: 318–321.

Briner, J.P., Kaufman, D.S., Werner, A., Caffee, M., Levy, L., Manley, W.F. et al. 2002. Glacier readvance during the Late Glacial (Younger Dryas?) in the Ahklun Mountains, southwestern Alaska. Geology, **30**: 679–682.

Carrara, P.E. 1987. Holocene and Latest Pleistocene glacial chronology, Glacier National Park, Montana. Canadian Journal of Earth Sciences, **24**: 387–395.

Carrara, P.E. 1989. Late Quaternary glacial and vegetative history of the glacier National Park region, Montana. US Geological Survey, Bulletin 1902.

Carrara, P.E., and McGimsey, R.G. 1988. Map showing distribution of moraines and extent of glaciers from the mid-19th Century to 1979 in the Mount Jackson area, Glacier National Park, Montana. US Geological Survey, Miscellaneous Investigations Series, map scale 1 : 24 000.

Carrara, P.E., and Trimble, D.A. 1992. A Glacier Peak and Mount Saint Helens J volcanic ash couplet and the timing of deglaciation in the Colville Valley area, Washington. Canadian Journal of Earth Sciences, **29**: 2397–2405.

Clark, D.H., and Gillespie, A.R. 1997. Timing and significance of Late-Glacial and Holocene cirque glaciation in the Sierra Nevada, California. Quaternary International, **38-39**: 21–38.

Dansgaard, W., White, J.W.C., and Johnsen, S.J. 1989. The abrupt termination of the Younger Dryas event. Nature, **339**: 532–533.

Davis, P.T., and Osborn, G. 1987. Age of Pre-Neoglacial cirque moraines in the central North American Cordillera. Géographie Physique et Quaternaire, **40**: 365–375.

Easterbrook, D.J., and Kovanen, D.J. 1998. New radiocarbon evidence for the ages of two Sumas moraines of the Cordilleran Ice Sheet between 10 000 and 11 30$^{0}$ $^{14}$C years BP. Geological Society of America, Abstracts with Programs, **30**: 165.

Engstrom, D.R., Hansen, B.C.S., and Wright, H.E., Jr. 1990. A possible Younger Dryas record in southeastern Alaska. Science, **250**: 1383–1385.

Fergusson, A., and Hills L.V. 1985. A palynological record, upper Elk Valley, British Columbia. *In* Climatic change in Canada 5. Critical periods in the Quaternary climatic history of northern North America. *Edited by* C.R. Harington. National Museum of Natural Sciences, Ottawa, Ont., pp. 355–369.

Ferguson, A., and Osborn, G. 1981. Minimum age of deglaciation of upper Elk Valley British Columbia. Canadian Journal of Earth Sciences, **18**: 1635–1636.

Franklin, F.F., Jr., Mehringer, P.J., Jr., and Sheppard, J.C. 1993. Age, distribution, and stratigraphy of Glacier Peak tephra in eastern Washington and western Montana, United States. Canadian Journal of Earth Sciences, **30**: 535–552.

Friele, P.A., and Clague, J.J. 2002. Younger Dryas readvance in Squamish River valley, southern Coast Mountains, British Columbia. Quaternary Science Reviews, **21**: 1925–1933.

Fulton, R.J. 1971. Radiocarbon geochronology of southern British Columbia. Geological Survey of Canada, Paper 71-37, pp. 28.

Fulton, R.J. 1984. Quaternary glaciation, Canadian Cordillera. *In* Quaternary stratigraphy of Canada. *Edited by* Fulton, R.J. Geological Survey of Canada, Paper 84-10, pp. 39–48.

Gardner, J.S. 1983. Observations on erosion by wet snow avalanches, Mount Rae area, Alberta, Canada. Arctic and Alpine Research, **15**: 271–274.

Gerloff, L.M., Hills, L.V., and Osborn, G.D. 1995. Post-glacial vegetation history of the Mission Mountains, Montana. Journal of Paleolimnology, **14**: 269–279.

Gosse, J.C., Evenson, E.B., Klein, J., Lawn, B., and Middleton, R. 1995. Precise cosmogenic $^{10}$Be measurements in western North America: support for a global Younger Dryas cooling event. Geology, **23**: 877–880.

Håkanson, L., and Jansson, M. 1983. Principles of lake sedimentology. Springer-Verlag, New York, N.Y.

Hallett, D.J., Hills, L.V., and Clague, J.J. 1997. New accelerator mass spectrometry radiocarbon ages for the Mazama tephra layer from Kootenay National Park, British Columbia, Canada. Canadian Journal of Earth Sciences, **34**: 1202–1209.

Harris, S.A., and Howell, J.A. 1977. Chateau Lake Louise moraines—Evidence for a new Holocene glacial event in southwest Alberta. Bulletin of Canadian Petroleum Geology, **25**: 441–455.

Heine, K. 1994. The Late-Glacial moraine sequences of Mexico; is there evidence for the Younger Dryas event? Palaeogeography, Palaeoclimatology, Palaeoecology, **112**: 113–123.

Heine, J.T. 1996. Evidence for a global Younger Dryas event on Mount Rainier Volcano, Washington? Geological Society of America, Abstracts with Programs, 77-46, p. F31.

Heine, K., and Heine, J.T. 1996. Late Glacial climatic fluctuations

© 2006 NRC Canada

in Ecuador; glacier retreat during Younger Dryas time. Arctic and Alpine Research, **28**: 496–501.

Heiri, O., Lotter, A.F., and Lemcke, G. 2001. Loss on ignition as a method for estimating organic and carbonate content in sediments: reproducibility and comparability of results. Journal of Paleolimnology, **25**: 101–110.

Kearney, M.S., and Luckman, B.H. 1987. A mid-Holocene vegetation and climate record from the subalpine zone of the Maligne valley, Jasper National Park Alberta, Canada. Palaeogeography, Palaeoclimatology, Palaeoecology, **59**: 227–242.

Kovanen, D.J. 2002. Morphologic and stratigraphic evidence for Allerød and Younger Dryas age glacier fluctuations of the Cordilleran Ice Sheet, British Columbia, Canada and northwest Washington, USA. Boreas, **31**: 163–184.

Kudras, H.R., Erienkeuser, H., Vollbrecht, R., and Weiss, W. 1991. Global nature of the Younger Dryas cooling event inferred from oxygen isotope data from Sulu Sea cores. Nature, **349**: 406–408.

Larsen, C.P.S., and MacDonald, G.M. 1993. Lake morphometry, sediment mixing and the selection of sites for fine resolution palaeoecological studies. Quaternary Science Reviews, **12**: 781–792.

Last, W.M., and Smol, J.P. 2001. Tracking environmental change using lake sediments. Vol. 2. Kluwer Academic Publishers, Dordrecht, The Netherlands.

Lemke, R.W., Mudge, M.R., Wilcox, R.E., and Powers, H.A. 1975. Geologic setting of the Glacier Peak and Mazama ash-bed markers in west-central Montana. United States Geological Survey, Bulletin 1395-H.

Luckman, B.H. 1975. Drop stones resulting from snow-avalanche deposition on lake ice. Journal of Glaciology, **14**: 186–188.

Luckman, B.H. 1988. 8,200 year old wood from the Athabasca Glacier, Alberta. Canadian Journal of Earth Sciences, **25**: 148–151.

Luckman, B.H., and Kearney, M.S. 1986. Reconstruction of Holocene changes in alpine vegetation and climate in the Maligne Range, Jasper National Park, Alberta. Quaternary Research, **26**: 244–261.

Luckman, B.H., and Osborn, G. 1979. Holocene glacier fluctuations in the middle Canadian Rocky Mountains. Quaternary Research, **11**: 52–57.

Mathewes, R.W., Heusser, L.E., and Patterson, R.T. 1993. Evidence for a Younger Dryas-like cooling event on the British Columbia coast. Geology, **21**: 101–104.

Mazzucchi, D., Spooner, I.S., Gilbert, R., and Osborn G. 2003. Reconstruction of Holocene climate change using multiproxy analysis of sediments from Pyramid Lake, British Columbia, Canada. Arctic, Antarctic and Alpine Research, **35**: 520–529.

McBirney, A.R. 1968. Compositional variations of the climatic eruption of Mount Mazama. *In* Andesite Conference Guidebook. *Edited by* H.M. Dole. Oregon Department of Geology and Mineral Industries, pp. 53–56.

Mehringer, P.J., Jr., Arno, S.F., and Petersen, K.L. 1977. Postglacial history of Lost Trail Pass Bog, Bitterroot Mountains, Montana. Arctic and Alpine Research, **9**: 345–368.

Menounos, B., and Reasoner, M.A. 1997. Evidence for cirque glaciation in the Colorado Front Range during the Younger Dryas chronozone. Quaternary Research, **48**: 38–47.

Menounos, B., Koch, J., Osborn, G., Clague, J., and Mazzuchi, D. 2004. Early Holocene glacier advance, southern Coast Mountains, British Columbia, Canada. Quaternary Science Reviews, **23**: 1543–1550.

Mikolajewicz, U., Crowley, T.J., Schiller, A., and Voss, R. 1997. Modelling teleconnections between the North Atlantic and North Pacific during the Younger Dryas. Nature, **387**: 384–387.

Nixon, D.J., and McClung, D.M. 1993. Snow avalanche runout from two Canadian mountain ranges. Annals of Glaciology **18**: 1–6.

Osborn, G. 1985. Holocene tephrostratigraphy and glacial fluctuations in Waterton Lakes and Glacier National Parks, Alberta and Montana. Canadian Journal of Earth Sciences, **22**: 1093–1101.

Osborn, G. 1986. Lateral moraine stratigraphy and Neoglacial history of Bugaboo Glacier, British Columbia. Quaternary Research, **26**: 171–178.

Osborn, G., and Gerloff, L. 1997. Latest Pleistocene and early Holocene fluctuations of glaciers in the Canadian and Northern American Rockies. Quaternary International, **38–39**: 7–19.

Osborn, G., Clapperton, C., Davis, P.T., Reasoner, M., Rodbell, D.T., Seltzer, G.O. et al. 1996. Potential glacial evidence for the Younger Dryas event in the Cordillera of North and South America. Quaternary Science Reviews, **14**: 823–832.

Reasoner, M.A. 1986. An inexpensive, lightweight percussion core sampling system. Géographie, physique et Quaternaire, **40**: 217–219.

Reasoner, M.A., Osborn, G., and Rutter, N.W. 1994. Age of the Crowfoot Advance in the Canadian Rocky Mountains: a glacial event coeval with the Younger Dryas oscillation. Geology, **22**: 439–442.

Rind, D., Peteet, D., Broecker, W., McIntyre, A., and Ruddiman, W. 1986. The impact of cold North Atlantic sea surface temperatures on climate: implications for the Younger Dryas cooling. Climate Dynamics, **1**: 3–33.

Rutter, N.W., Weaver, A.J., Rokosh, D., Fanning, A.F., and Wright, D.G. 2000. Data-model comparison of the Younger Dryas event. Canadian Journal of Earth Sciences, **37**: 811–830.

Ryder, J.M., and Thomson, B. 1986. Neoglaciation in the southern Coast Mountains of British Columbia: chronology prior to the late-Neoglacial maximum. Canadian Journal of Earth Sciences, **23**: 237–238.

Scott, L., Steenkamp, M., and Beaumont, B.P. 1995. Palaeoenvironmental conditions in South Africa at the Pleistocene-Holocene transition. Quaternary Science Reviews, **14**: 937–947.

Singer, C., Shulmeister, J., and McLean, B. 1998. Evidence against a significant Younger Dryas cooling event in New Zealand. Science, **281**: 812–814.

Smith, I.R. 2000. Diamictic sediments within high Arctic Lake sediment cores: evidence for lake ice rafting along the lateral glacial margin. Sedimentology, **47**: 1157–1179.

Spooner, I.S., Hills, L.V., and Osborn, G.D. 1997. Reconstruction of Holocene Changes in alpine vegetation and climate, Susie Lake, British Columbia, Canada. Arctic and Alpine Research, **29**: 156–163.

Spooner, I.S., Mazzuchi, D., Osborn, G., Gilbert, R., and Larocque, I. 2002. A multi-proxy Late Pleistocene and Holocene record of sediment of Skinny Lake, Iskut region, northern British Columbia, Canada. Journal of Paleolimnology, **28**: 419–431.

Taylor, K.C., Lamorey, G.W., Doyle, G.A., Alley, R.B., Grootes, P.M., Mayewski, P.A.et al. 1993. The "flickering switch" of Late Pleistocene climate change. Nature, **361**: 432–435.

Thompson, R., Battarbee, R.W., O'Sullivan, P.E., and Oldfield, F. 1975. Magnetic susceptibility of lake sediments. Limnology and Oceanography, **20**: 687–698.

Tomkins, J. 2000. Regional Holocene climate of Alberta and northwestern Montana through lake core sediment analysis. B.Sc. thesis, University of Calgary, Calgary, Alberta.

Waitt, R.B., Jr., and Thorson, R.M. 1983. The Cordilleran Ice Sheet in Washington, Idaho and Montana. *In* Late Quaternary environments of the United States. *Edited by* H.E. Wright and S.C. Porter. University of Minnesota Press, Minneapolis, Minn., Vol. 1, pp. 53–70.

© 2006 NRC Canada

Westgate, J.A., and Gorton, M.P. 1981. Correlation techniques in tephra studies. *In* Tephra studies. *Edited by* S. Self and R.J. Sparks. D. Reidel Publishing, Dordrecht, The Netherlands, pp. 73–94.

Zhou, W., Head, M.J., An, Z., Deckker, P.D., Liu, Z., Liu, X. et al. 2001. Terrestrial evidence for a spatial structure of tropical-polar interconnections during the Younger Dryas episode. Earth and Planetary Science Letters, **191**: 231–239.

Zielinski, G.A., and Davis, P.T. 1987. Late Pleistocene age for the type Temple Lake moraine, Wind River Range, Wyoming, USA. Géographie Physique et Quaternaire, **41**: 397–401.

© 2006 NRC Canada